

# An Efficient Method for Modeling Parasitic Light Sensitivity in Global Shutter CMOS Image Sensors

Federico Pace<sup>1,2</sup>, Olivier Marcelot<sup>1</sup>, Philippe Martin-Gonthier<sup>1</sup>, Olivier Saint-Pé<sup>2</sup>, Michel Breart de Boisanger<sup>2</sup>, Rose-Marie Sauvage<sup>3</sup> and Pierre Magnan<sup>1</sup>

<sup>1</sup>ISAE-SUPAERO, Université de Toulouse, 10 Avenue Edouard Belin, 31055 Toulouse, France

<sup>2</sup>Airbus Defence & Space, 31 Rue des Cosmonautes, ZI du Palais, 31400 Toulouse, France

<sup>3</sup>Direction Générale de l'Armement, 60 Boulevard du Général Martial Valin, 75509 Paris, France

E-mail: federico.pace@isae-supaero.fr, Tel: +33 5 61 33 87 94

**Abstract**—Parasitic Light Sensitivity (PLS) is a key performance parameter for Global Shutter CMOS Image Sensors (GS-CIS), which quantifies the sensor sensitivity to light when the shutter is supposed closed. Its modeling and understanding would allow for an optimization in developing future sensors. This paper aims to present an efficient method for 2D modeling PLS in GS-CIS through separation of the optical problem from the carriers motion one. The optical problem is solved thanks to Finite-Differences Time-Domain (FDTD) simulations, while solution to the carriers motion problem is given through the application of the Boltzmann Transport Equation (BTE). This method is presented as a faster alternative to the coupled use of FDTD and TCAD simulations: since it is supposed that the two problem solutions are independent, the two simulations can be performed in parallel. The results show good match between the developed method and the TCAD solutions, thus showing fair agreement with experimental data, probably due to a poor knowledge of the back-end process.

**Index Terms**—CIS, GS, FDTD, BTE, PLS, Shutter Efficiency

## I. INTRODUCTION

Global Shutter CMOS Image Sensors (GS-CIS) [1]–[4] are increasingly becoming attractive for a wide spectrum of appli-

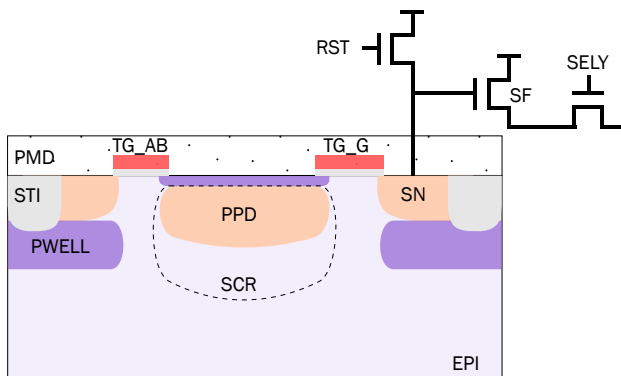


Fig. 1. Example of a GS 5T pixel cross section. Pinned PhotoDiode (PPD) is visible at the center of the figure with its pinning layer (depicted in violet just above). Storage Node (SN) is situated right to the PPD and acts also as the Floating Diffusion (FD) of the 5T GS-CIS. Transfer Gate is of Global type (TG\_G) and an Anti-Blooming Transfer Gate (TG\_AB) is visible at the left-hand side of the figure.

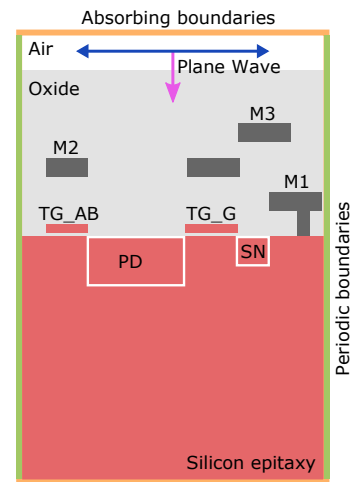


Fig. 2. Example of the structure simulated with the FDTD method. As a case of study, only M3 is used in the pixel to screen the SN. Blue line shows one of the two simulated Plane Wave polarization. Only normal light incidence has been simulated for this study, but oblique light incidence could also be considered. Structure of pixel can also be appreciated.

cations, ranging from automotive [5] to space applications [6], having been conceived for reducing motion artifacts.

An example of a pixel that can operate in Global Shutter mode is presented in Fig. 1. In Global Shutter mode, the incoming light gets collected by the PhotoDiode (PD) for a certain amount of time, then the stored charges are transferred from the PD to the Sense Node (SN) in a synchronous way throughout the entire matrix and stored for readout. Due to the matrix dimensions, synchronous global readout of the stored signal is not feasible, thus requiring a rolling-shutter fashion readout that is performed line by line. Given that the SN sensitivity to parasitic charges is non-negligible, there could appear some unwanted signal that is not constant throughout the entire matrix and degrade the Global Shutter performances.

In order to evaluate the system capacity to screen the SN from external perturbations, a figure of merit has been identified, defined as Parasitic Light Sensitivity (PLS), and

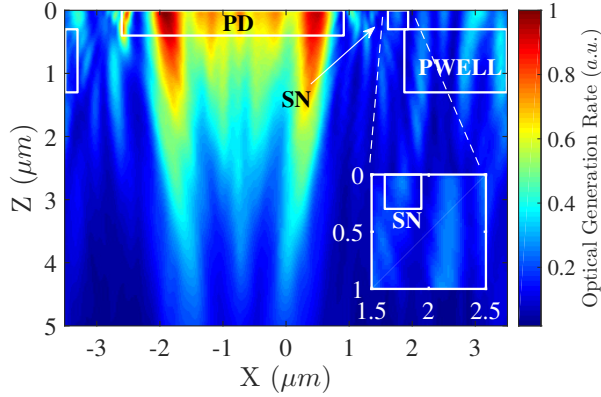


Fig. 3. Example of Optical Generation Rate map at  $\lambda = 650 \text{ nm}$ . The map extends in the  $z$ -direction from  $0 \mu\text{m}$  (silicon surface) to  $5 \mu\text{m}$  (end of silicon epitaxy). Zoom in the SN region is also shown. Non-negligible generation rate is found in and close to the SN zone. Screening of pixel is therefore not perfect because of light diffraction, becoming increasingly important in smaller pixels and that has to be taken into account when designing GS-CIS.

described in (1), with  $S_m$  being the sensitivity of node  $m$ .

$$PLS = S_{SN}/S_{PD} \quad (1)$$

Since limited work has been proposed so far and only for specific cases, such as BackSide Illumination pixels or just PLS simulation results without explanation of the method [7], [8], this paper aims to propose a faster alternative 2D method to TCAD simulations for modeling PLS in GS-CIS. Results are shown for a  $7 \mu\text{m}$  pitch pixel and compared to TCAD simulations, knowing that the method can be applied to a large variety of pixel dimension and structures.

## II. METHOD FOR MODELING PLS

The presented 2D method exploits Finite-Differences Time-Domain (FDTD) simulations for photo-generation of carriers and aims to treat carriers motion through Boltzmann Transport Equation (BTE). Silicon has a negligible thermal recombination at moderate illumination strengths, carriers transport is supposed independent on the carriers density thus transport problem and optical problem can be considered uncorrelated. This brings some advantages in terms of computational time in comparison with TCAD simulations:

- it allows running the optical and the carrier transport simulations in parallel, which would not be possible when exploiting TCAD simulations because the optical problem solution must be given as input to perform the carrier transport simulation;
- it allows running a lesser number of simulation when optical conditions are to be changed (for example incidence angle, light intensity, etc.), there is no need in re-performing the carrier transport simulations.

In a general case, this method can be preferred to TCAD simulation for a faster analysis of the device in various conditions.

The following will briefly describe the formulation and the solution of the two problems previously stated.

### A. Photo-Generation of Carriers

In order to solve the optical problem and calculate the photo-generation rate, a commercial software exploiting the FDTD method has been exploited [9]. The FDTD method is generally used to solve Maxwell's equations for light in visible and near-visible wavelength range through use of a rectangular finite-difference mesh [10], [11].

Fig. 2 shows an example of the FDTD simulated pixel structure. In order to reproduce the behavior of a pixel inside a matrix, periodic boundary conditions of the Bloch type are applied on the right-hand side and left-hand side of the simulated structure, where it is supposed identical pixels would take place. On the other hand, absorbing boundary conditions are placed at the bottom of the silicon epitaxy and at the top of the simulates structure. It is therefore supposed that all the light reflected by the pixel or the light moving towards the substrate (below the epitaxy) would not be useful for our simulation. Plane Waves with normal incidence has been used for the presented simulation, even though other incidence angle could also be tested. Non-polarized light has been achieved through averaging of two orthogonal polarization simulations. Source incoherence has been achieved through spectral averaging.

The simulations result in an Optical Generation Rate Density (OGRD) map per each considered wavelength, describing the photo-electron generation rate density per each point at the epitaxial silicon level. An example of OGRD is shown in Fig. 3. It is possible to appreciate that non-negligible direct light is coming onto the SN because of diffraction and multiple reflections.

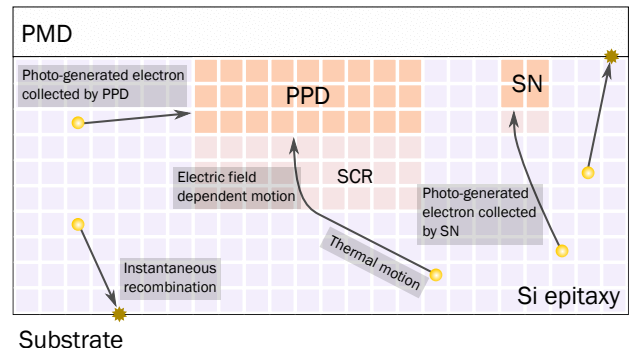


Fig. 4. Example of simulation exploiting the Boltzmann Transport Equations under the given hypothesis. A carrier is created in a voxel, its initial direction is randomly chosen. Then, electron moves according to the BTE. The electron motion is not perturbed by any scattering nor recombination effects, except when reaching a simulation border (silicon/PMD interface for example) where its recombination is instantaneous and considered lost. Electron motion also ends when reaching the PD or SN node, and the electron is taken into account for the arrival node.

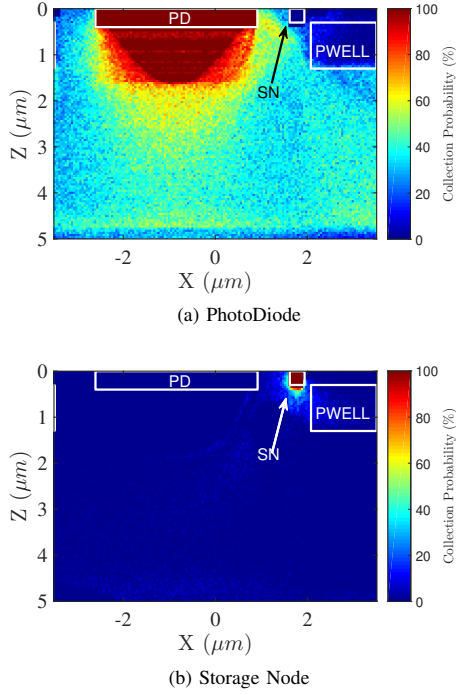


Fig. 5. Example of Collection Probability map of (a) PD and (b) SN, simulated with the Boltzmann Transport Equations at  $\lambda = 650 \text{ nm}$ . In (b) it is possible to appreciate non-negligible collection probability far from the SN zone, showing the interest in our study.

### B. Photo-Generated Carriers Motion

BTE is used to model the behavior of particles in semiconductors under non-equilibrium state as function of time and the local electric field [12], [13].

As for the assumptions, no scattering has been taken into account, as well as instantaneous recombination at surfaces and wavelength dependent initial carrier energy. These assumptions bring to the behavior represented in Fig. 4.

BTE are then used to create a Collection Probability (CP) map for both PD and SN. A CP map describes the probability of a carrier, created at a point in space, to be collected by either the PD or the SN. For this purpose, 100 carriers per point in space are simulated. Fig. 5 shows an example of CP map for the PD.

The OGRD and CP maps are finally used to compute the nodes sensitivity  $\mathcal{S}$  through (2) per each wavelength. Since simulations are performed in 2D, a geometry correction factor has to be applied and it has been identified in the node's third dimension ( $w_{PD}$  and  $w_{SN}$  for PD and SN respectively). Finally, the desired PLS can be computed through (3).

$$\mathcal{S}_{PD} = w_{PD} \cdot \iint \text{OGRD} \cdot \text{CP}_{PD} \cdot dx dz, \quad (2)$$

$$\mathcal{S}_{SN} = w_{SN} \cdot \iint \text{OGRD} \cdot \text{CP}_{SN} \cdot dx dz$$

$$\text{PLS} = \frac{\mathcal{S}_{SN}}{\mathcal{S}_{PD}} = \frac{w_{SN} \cdot \iint \text{OGRD} \cdot \text{CP}_{SN} \cdot dx dz}{w_{PD} \cdot \iint \text{OGRD} \cdot \text{CP}_{PD} \cdot dx dz} \quad (3)$$

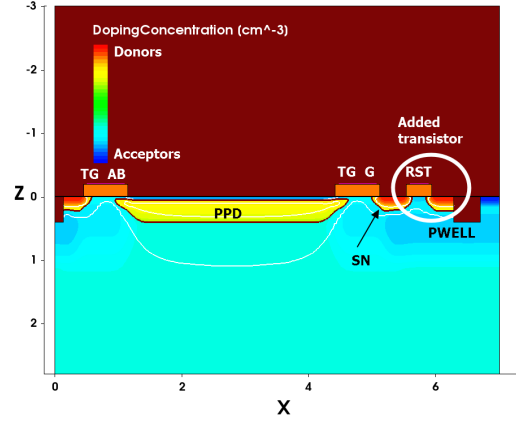


Fig. 6. Example of the pixel structure simulated exploiting TCAD, here represented thanks to doping concentration. White lines represent boundaries of Space Charge Regions (SCR) when the PPD is emptied. As it can be appreciated in the white circle, a transistor is added in order to allow the SN to be floating.

### III. COUPLED FDTD+TCAD SIMULATIONS

As reference, TCAD simulations have been exploited. In order to start from the same optical assumptions, optical generation data from Lumerical have been imported to the TCAD simulator (for our purposes Synopsys Sentaurus has been used) through a MATLAB routine using a linear interpolation from the finite difference mesh to the finite element one [14].

The 2D simulated structure is shown in 6. It can be appreciated that an additional transistor (i.e. RST) has to be added in order to allow the potential of the SN to be floating. However, in some pixel structures the RST transistor can be placed distant in space from the SN node and connected to the latter via a metallic connection; 3D TCAD simulations become necessary to correctly simulate the floating behavior of the SN.

PD and SN sensitivities are calculated through the slope of the electron density change, in the nodes, as function of time.

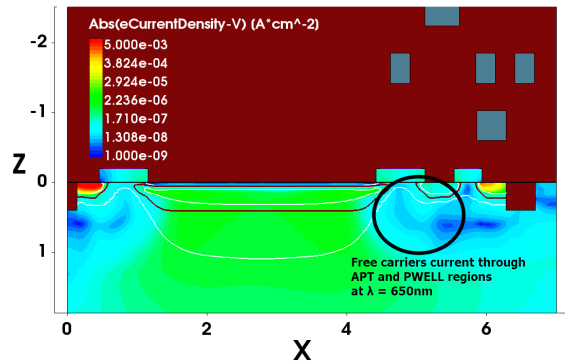


Fig. 7. Absolute electron current density while under illumination at  $\lambda = 650 \text{ nm}$ . It is possible to appreciate how the main electronic current flowing towards the SN (shown by the black circle) passes close to the PWELL region, where p-doping decreases.

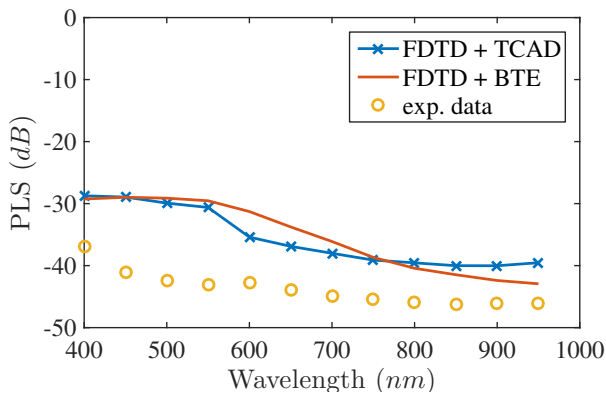


Fig. 8. PLS simulation results are shown for both coupled FDTD+TCAD simulations and FDTD+BTE method. A good agreement of the results can be appreciated between the two methods, although simulations show discrepancies with the experimental data curve. As for the experimental part, node's sensitivity is measured through variation of its output voltage as function of the impinging light irradiance. PLS is finally calculated as the ratio of the two sensitivities.

PLS is then calculated using (3).

Moreover, a further comparison of the two methods could be done. Taking a look at the absolute electronic current flow in the pixel resulting from TCAD simulations in Fig. 7, it is possible to appreciate that the main current flowing towards the SN comes from free carriers close to the end of the PWELL area, where the Anti-PunchThrough (APT) region is present and being lightly doped compared to the PWELL region. Similarly, it can be appreciated from Fig. 5b that the probability of carriers being collected by the SN is non-negligible in the same region explained for TCAD simulations.

#### IV. SIMULATION RESULTS AND EXPERIMENTAL DATA

Figure 8 shows the comparison between the coupled FDTD+TCAD simulation and our method exploiting FDTD simulations and BTE. Our model shows good match to the TCAD modeling, with a similar behavior in the entire tested wavelength range.

The simulations results have moreover been compared with experimental data taken from a matrix of  $7 \mu\text{m}$  pitch pixels with Global Shutter functions, on which the simulated structure have been modeled. As it can be appreciated in Fig. 8, simulations show some discrepancies with the experimental data, the reason still being under investigation. One hypothesis is that the discrepancy can be caused by poor knowledge in the Back-End fabrication process, where diverse oxide layers can strongly modify the propagation of light inside the pixel and thus modify the optical generation pattern at the silicon level. This can be especially justified from the fact that the discrepancy is stronger at shorter wavelength, where light penetration is mainly superficial and carriers diffusion has a lesser impact.

#### V. CONCLUSIONS

We have presented a new method for modeling PLS in GS-CIS. The method shows its interest when used to model PLS at

different optical condition (e.g. incidence angle, light intensity, ...). Compared to coupled FDTD+TCAD simulations, where a TCAD simulation has to be done per each optical condition, our model results faster, where only FDTD simulations have to be re-performed, and allows parallelization, showing the interest in our study.

Simulation results have been moreover compared to experimental data, showing some discrepancies, especially at longer wavelengths. This could be explained by a poor knowledge in the Back-End fabrication process.

Finally, our method could be further improved by creating a more realistic electric field chart for BTE calculations and with a better comprehension and modeling of the Back-End layers. 3D simulations could also improve results, taking into account the complexity of the pixel structure.

#### REFERENCES

- [1] G. Meynants, J. Bogaerts, X. Wang, and G. Vanhorebeek, "Backside illuminated global shutter CMOS image sensors," in *Int. Image Sensor Workshop (IISW)*, 2011, pp. 305–308.
- [2] A. Krymski, "A High Speed 1 MPix Sensor with Floating Storage Gate Pixel," *Proc. Int. Image Sensor Workshop (IISW)*, 2015.
- [3] S. Velichko, J. J. Hyneczek, R. S. Johnson, V. Lenchenkov, H. Komori, H. W. Lee, and F. Y. J. Chen, "CMOS Global Shutter Charge Storage Pixels With Improved Performance," *IEEE Transactions on Electron Devices*, vol. 63, no. 1, pp. 106–112, Jan. 2016.
- [4] M. Kobayashi, Y. Onuki, K. Kawabata, H. Sekine, T. Tsuboi, T. Muto, T. Akiyama, Y. Matsuno, H. Takahashi, T. Koizumi, K. Sakurai, H. Yuzurihara, S. Inoue, and T. Ichikawa, "A  $1.8e^{-6}$  rms  $5 \mu\text{s}$  Temporal Noise Over 110-dB-Dynamic Range  $3.4 \mu\text{m}$  Pixel Pitch Global-Shutter CMOS Image Sensor With Dual-Gain Amplifiers SS-ADC, Light Guide Structure, and Multiple-Accumulation Shutter," *IEEE Journal of Solid-State Circuits*, vol. 53, no. 1, pp. 219–228, Jan. 2018.
- [5] A. Lahav, A. Birman, D. Perhest, A. Fenigstein, Y. Grauer, and E. Levi, "A global shutter sensor used in active gated imaging for automotive," in *Proc. IISW*, 2015, pp. 1–4.
- [6] G. Lepage, A. Materne, and C. Renard, "A CMOS image sensor for Earth observation with high efficiency snapshot shutter," in *Proc. Int. Image Sensor Workshop (IISW)*, 2013.
- [7] L. Stark, J. M. Raynor, F. Lalanne, and R. K. Henderson, "A Back-Illuminated Voltage-Domain Global Shutter Pixel With Dual In-Pixel Storage," *IEEE Transactions on Electron Devices*, vol. 65, no. 10, pp. 4394–4400, Oct. 2018.
- [8] T. Yokoyama, M. Tsutsui, M. Suzuki, Y. Nishi, I. Mizuno, and A. Lahav, "Development of Low Parasitic Light Sensitivity and Low Dark Current  $2.8 \mu\text{m}$  Global Shutter Pixel," *IEEE Sensors*, vol. 18, no. 2, p. 349, Jan. 2018. [Online]. Available: <http://www.mdpi.com/1424-8220/18/2/349>
- [9] Lumerical Inc. [Online]. Available: <https://www.lumerical.com/>
- [10] K. Yee, "Numerical solution of initial boundary value problems involving maxwell's equations in isotropic media," *IEEE Transactions on Antennas and Propagation*, vol. 14, no. 3, pp. 302–307, May 1966.
- [11] J. Vaillant, A. Crocherie, F. Hirigoyen, A. Cadien, and J. Pond, "Uniform illumination and rigorous electromagnetic simulations applied to CMOS image sensors," *Optics Express*, vol. 15, no. 9, pp. 5494–5503, 2007.
- [12] C. Jacoboni and L. Reggiani, "The Monte Carlo method for the solution of charge transport in semiconductors with applications to covalent materials," *Rev. Mod. Phys.*, vol. 55, no. 3, pp. 645–705, Jul. 1983. [Online]. Available: <https://link.aps.org/doi/10.1103/RevModPhys.55.645>
- [13] Y. Yamashita, M. Uchiyama, and D.-N. Yaung, "Quantum Efficiency Simulation with Boltzmann Transport Equation for Motion Modeling of Individual Particles in Photodiodes," *Proc. Int. Image Sensor Workshop (IISW)*, 2017.
- [14] M. D. Kelzenberg, *Silicon microwire photovoltaics*. California Institute of Technology, 2010.